Int J Cardiovasc Imaging (2011) 27:289–298
DOI 10.1007/s10554-010-9790-1

ORIGINAL PAPER

Plaque and thrombus evaluation by optical coherence tomography

Takashi Kubo · Chenyang Xu · Zhao Wang · Nienke S. van Ditzhuijzen · Hiram G. Bezerra

Received: 10 December 2010 / Accepted: 30 December 2010 / Published online: 19 February 2011

Abstract Intravascular Optical Coherence Tomography has been explored as an imaging tool for vessel wall and thrombus characterization. OCT enables a high resolution arterial wall imaging, and light properties allow tissue characterization. It has been proved one of the most valuable imaging modalities for the evaluation of vulnerable plaque and thrombus. OCT has a unique capacity in volumetric quantification of calcium, and unlike ultrasound, light can easily penetrate calcified plaques. Finally, this review paper will address aspects of the validation method of plaque characterization and potential pitfalls and put in perspective new approaches that may help the evolution of the field.

Keywords Optical coherence tomography · Atherosclerosis · Plaque · Imaging

Hiram G Bezerra received honoraria grant from St. Jude Medical.

T. Kubo
Department of Cardiovascular Medicine, Wakayama Medical University, Wakayama, Japan

C. Xu
Lightlab Imaging Inc., Westford, MA, USA

Z. Wang
Department of Biomedical Engineering, Case Western Reserve University, Cleveland, OH, USA

N. S. van Ditzhuijzen · H. G. Bezerra (✉)
Harrington-McLaughlin Heart and Vascular Institute, Cardiovascular Imaging Core Laboratory, University Hospitals Medical Center, Case Western Reserve University School of Medicine, Cleveland, OH, USA
e-mail: hiram.bezerra@UHhospitals.org

Plaque classification

Since the inventors of Optical Coherence Tomography initially proposed that OCT could be used for visualizing atherosclerosis [1], there have been continuous efforts to correlate features of OCT images with histopathological plaque types. The initial OCT studies on artery tissues were performed in mid-90's on post-mortem aorta samples, where the properties of fibroatheroma and fibrocalcific plaques were first described [2]. In 2002, Yabushita et al. published a qualitative image classification scheme based on correlation of OCT images with histology images of a large series of autopsy specimens [3]. The fibrous tissue was characterized as homogeneously signal-rich regions, calcified tissue as heterogeneous, signal-poor regions with sharp borders, and lipid tissue as homogeneously signal-poor regions with diffuse borders. Later, Jang et al. proposed a similar scheme based on results of in vitro studies and confirmed that the same criteria were applicable to in vivo imaging by comparing the OCT images to Intravascular Ultrasound (IVUS) images [4]. It was also reported that the macrophage foam cells could be detected and quantified with high accuracy

[5]. These qualitative observations were further confirmed by a number of other studies and have become the basis for the *de facto* standard for visual characterization of OCT images [6–8].

Using these qualitative criteria, initial in vitro studies showed that the coronary lesions can be classified with average sensitivities and specificities in the 70–90% range. This level of accuracy, although higher than some other imaging methods, still needs improvement before these criteria can be applied for routine clinical decision-making. In addition, the mechanisms on which these qualitative observations are based have not been fully explained and several deficiencies need to be addressed. For example, the measurement of fibrous cap thickness, an uttermost important parameter for assessing plaque vulnerability, is ill-defined using these criteria. Although there is a well-delineated border between fibrous cap and the lipid pool in histology, the location of this border cannot be identified precisely in OCT if the lipid pool is "diffusely bordered". Instead, researchers have to rely on extensive experience and deep understanding of OCT images to identify the thin-capped fibroatheromas (TCFAs) [9, 10].

To improve the tissue characterization, both hardware and software approaches have been investigated. To increase the image contrast between the fibrous cap and the lipid tissue, polarization-sensitive OCT systems have been developed for measurement of the tissue birefringence [11, 12]. The concept underlying polarization-sensitive imaging is that, because they tend to be highly organized and anisotropic, collagen fiber bundles and smooth muscle cells are more birefringent than other disorganized plaque components, such as the lipid tissue. However, birefringence can only be measured accurately over a relatively large distance (e.g., 200 μm), which is insufficient for characterizing the thin fibrous cap (<65 μm) in the vulnerable plaques.

As is the case for any new imaging method, the utility of qualitative OCT observation can be greatly enhanced if the fundamental physical explanations can be found. Without such theoretical explanation, the OCT images are prone to misinterpretation. According to the single-scattering theory, the intensity of OCT signal $I(z)$ of a homogeneous tissue at depth z is

$$I(z) = A(z)\mu_b \exp(-\mu_t z/n),$$

where $A(z)$ represents the efficiency of OCT system, the μ_b is the backscattering coefficient, μ_t is the total attenuation coefficient and n is the refractive index. Attempts to measure the scattering coefficient and attenuation coefficients were first performed by imaging post-mortem arteries from lumen side with varying results [13, 14]. However, because the plaques usually are multi-layered, it is difficult to exactly match the histology to the corresponding OCT images. Xu et al. introduced the idea of measuring optical properties of transversely sectioned arteries, in which each plaque component could be exposed and easily registered to histology [15]. Figure 1 shows the transversely scanned OCT images, the corresponding rotary OCT scanning images, and histology images of a representative fibroatheroma and a fibrocalcific plaque. Although the rotary OCT images were consistent with the previously published qualitative criteria, the transversely scanned OCT images showed that the lipid region appeared to be signal-rich at the top layer, and only became signal-poor at deeper layers as the result of high signal attenuation. The light backscattering coefficient μ_b and attenuation coefficients μ_t were determined for calcified tissue ($\mu_b = 4.9 \pm 1.5\ \text{mm}^{-1}$, $\mu_t = 5.7 \pm 1.4\ \text{mm}^{-1}$), fibrous tissue ($\mu_b = 18.4 \pm 6.4\ \text{mm}^{-1}$, $\mu_t = 6.4 \pm 1.2\ \text{mm}^{-1}$), and lipid tissue ($\mu_b = 28.1 \pm 8.9\ \text{mm}^{-1}$, $\mu_t = 13.7 \pm 4.5\ \text{mm}^{-1}$). The attenuation coefficients μ_t was also measured from rotary OCT images with similar results (healthy vessel wall and intimal thickening: 2–5 mm^{-1}, necrotic core: >10 mm^{-1}, macrophage infiltration: >12 mm^{-1}) [16].

Quantitative analysis offered new insights to the interpretation of OCT images. Table 1 summarizes the OCT image features of main coronary artery tissue types. However, there are still limitations with this approach. Because the attenuation, similar to birefringence, is also a range-derived parameter, it can only be measured over a distance. Averaging of neighboring scan lines is also required to reduce the effect of speckle noise. Hence, the effective spatial resolution for optical parameter extraction is compromised. With the advance of the fast frequency-domain OCT system and improved resolution, such measurement may become more reliable and may offer further cues to identification of TCFA.

OCT might be the best tool available to detect vulnerable plaque (Fig. 2). To assess the ability of each imaging method to detect the specific characteristics of vulnerable plaque, Kubo et al. [10]

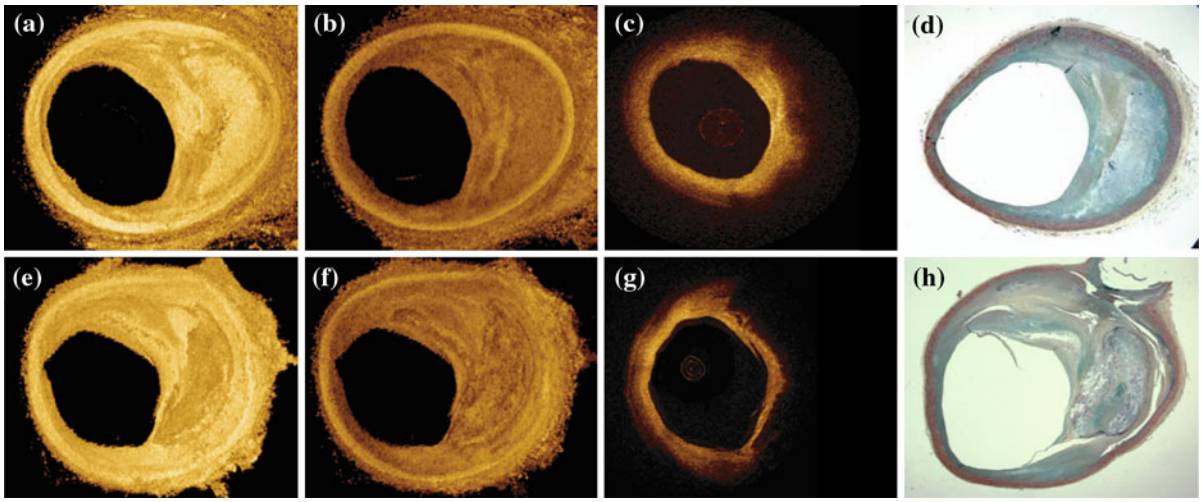

Fig. 1 Comparison of transverse OCT images at 50 μm (**a**, **e**) and 500 μm (**b**, **f**) below the surface, with corresponding rotary OCT image (**c**, **g**) and corresponding histology (Movat's pentachrome) (**d**, **h**) for a representative fibrolipid plaque (*top row*) and a fibrocalcific plaque (*bottom row*). A consistent color map was used for **a**, **b**, **c**, **e**, **f**, **g**

Table 1 OCT image features of main coronary artery tissue types

Histopathologic features	OCT features
Fibrous tissue	Homogeneous, signal-rich, birefringent
Calcification tissue	Heterogeneous, sharply bordered, signal-poor
Lipid-rich tissue	Signal-rich at the top, high-attenuation regions
Macrophage foam cells	Heterogeneous, lumpy, signal rich, very high attenuation
Intima	Signal-rich layer near lumen
Media	Signal-poor middle layer
Adventitia	Signal-rich, heterogeneous outer layer

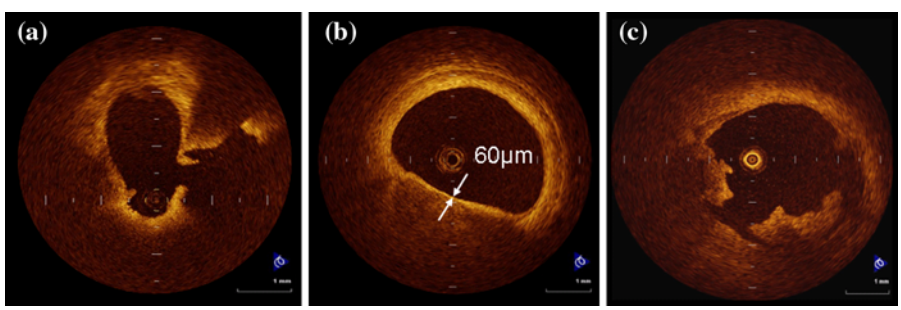

Fig. 2 OCT images of vulnerable plaques **a** Plaque rupture. **b** Thin-capped fibroatheroma (Fibrous-cap thickness = 60 μm). **c** Intracoronary thrombus

performed OCT, IVUS and angioscopy in patients with acute myocardial infarction. OCT was superior in detecting plaque rupture (73% vs. 40% vs. 43%, $P = 0.021$), erosion (23% vs. 0% vs. 3%, $P = 0.003$) and thrombus (100% vs. 33% vs. 100%, $P < 0.001$) as compared to IVUS and angioscopy. Intra- and inter-observer variability yielded acceptable concordance for these characteristics ($\kappa = 0.61$–0.83). The high resolution of OCT allows us to identify the thin fibrous cap (<65 μm) in vivo. Kume et al. [17]

examined the reliability of OCT for measuring the fibrous cap thickness. In the examination of 35 lipid-rich plaques from 38 human cadavers, there was a good correlation of the fibrous cap thickness between OCT and histological examination ($r = 0.90$; $P < 0.001$). Sawada et al. [9] evaluated the feasibility of OCT and virtual histology IVUS for detecting thin-capped fibroatheroma (TCFA). Although the positive ratio of virtual histology IVUS for detecting TCFA was 45.9%, that of OCT was 77.8%. Kubo et al. [18] assessed the relationship between plaque color evaluated by coronary angioscopy and fibrous cap thickness estimated by OCT. There was a significant negative correlation between yellow color intensity and fibrous cap thickness ($P < 0.0001$), and all of the OCT-derived TCFAs showed intensive yellow color. Kashiwagi et al. [19] evaluated culprit lesions in acute coronary syndrome by both OCT and multidetector computed tomography. OCT-derived TCFAs had significantly lower computed tomography attenuation values in the culprit plaque compared to non-TCFAs (35.1 ± 32.3 HU vs. 62.0 ± 33.6 HU, $P < 0.001$). Jang et al. [6] analyzed OCT images among 57 patients who presented with stable angina pectoris (SAP), acute coronary syndrome (ACS), or AMI. The AMI group was more likely than the ACS group, who was more likely than the SAP group, to have a thinner cap, more lipid, and a higher percentage of TCFA (72% vs. 50% vs. 20%, respectively, $P = 0.012$). Fujii et al. [20] performed a prospective OCT analysis of all 3 major coronary arteries to evaluate the incidence and predictors of TCFAs in patients with AMI and SAP. Multiple TCFAs were observed more frequently in AMI patients than in SAP patients (69 vs. 10%, $P < 0.001$). In the entire cohort, multivariate analysis revealed that the only independent predictor of TCFA was AMI (OR = 4.12, 95% CI = 2.35–9.87, $P = 0.02$). The OCT characteristics of coronary thrombi were studied by Kume et al. [21] in 108 coronary arterial segments at postmortem examination. White thrombi were identified as signal-rich, low-backscattering protrusions in the OCT image, while red thrombi were identified as high-backscattering protrusions inside the lumen of the artery, with signal-free shadow. Using a measurement of the OCT signal attenuation within the thrombus, the authors demonstrated that a cut-off value of 250 μm in the 1/2 width of signal attenuation can differentiate white from red thrombi with a high sensitivity (90%) and specificity (88%).

Coronary calcification

Calcification of coronary arteries is an important marker of atherosclerosis, and the amount of calcification is associated with total plaque burden [22–24]. Calcium measurement is usually performed non-invasively by electron beam computed tomography (EBCT [25, 26]) and multidetector computed tomography (MDCT [26]), or invasively by intravascular ultrasound (IVUS). Calcified lesions can be detected by OCT with high sensitivity (96%) and specificity (97%) [3]. Calcium is seen as a hypo-signal region delineated by a sharp boundary [3]. The advantage of OCT over other imaging modalities for calcium assessment is its ability for three-dimensional volumetric calcium characterization, which cannot be obtained by IVUS due to the limited penetration of ultrasound in calcified lesions [24]. Although EBCT could indirectly evaluate the calcium volume by isotropic interpolation [27], its low resolution (~1 mm) prevents accurate morphological assessment. OCT has unique advantages for coronary calcium assessment. It provides the highest resolution with better light penetration in calcium as compared to IVUS. The presence and extent of superficial calcifications can strongly affect the success rate of percutaneous coronary intervention (PCI) [28] causing stent under-expansion and associated stent thrombosis. Therefore, OCT can be used for collecting information on the amount of calcium and distance from the lumen, ultimately debunking techniques like rotational atherectomy and cutting-balloon can be applied [29].

Whether for general volumetric calcium assessment, or for determining the depth and extent of calcification before PCI, an accurate automatic method is important, especially when OCT moves to the clinical bedside, where manual analysis of large amount of data is impractical. The automatic calcium assessment can be thought of consisting of two parts: calcium detection and quantification. Accurate quantification relies on good segmentation, where any clinically relevant quantitative measures can be derived, such as area, depth, arc and thickness in individual frames, and volume along the selected

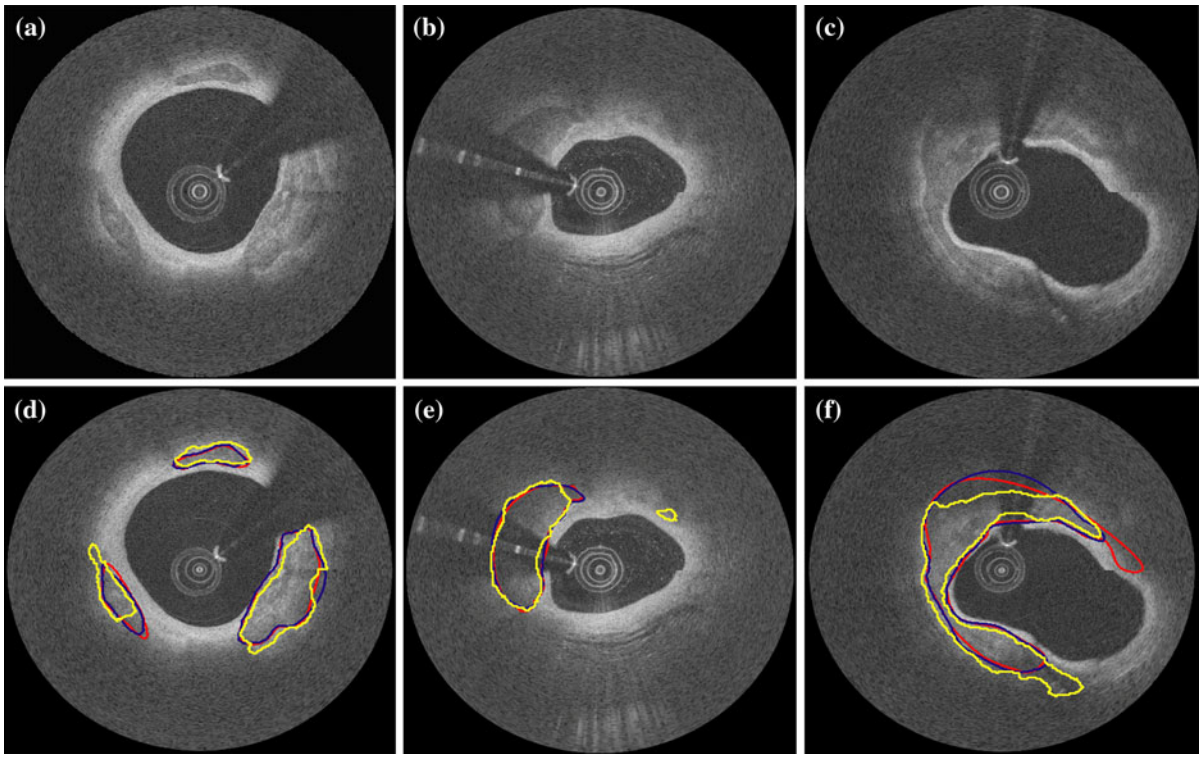

Fig. 3 Automatic segmentation of calcified plaques (CP). **a**–**c** Original images. **d**–**f** Corresponding manual and automatic segmentation results. *Red* manual segmentation by observer 1, *blue* manual segmentation by observer 2, *yellow* automatic method. The CP in **c** has unclear border and the CPs in **b** and **c** are blocked by the guide wire. A false positive region is also shown in **e** (1–2 o'clock)

coronary portion. A semi-automatic segmentation method was developed by our group [30]. The calcified plaques were located by edge detection after automatic segmentation of lumen, guide wire and arterial wall. Based on an active contour model using level sets, an initial contour generated from the binary edge image was driven to the calcium boundary of high gradient and maximized intensity differences between the region outside and inside the contour. The algorithm could guess the missing boundary when the calcified plaques were blocked by the guide wire or when the outer boundary was obscured due to signal drop-off (Fig. 3). For a variety of calcified plaques, the automatic method achieved accuracy around 80% as compared to "ground truth" manual segmentation. More efforts are being put to incorporate a separate calcium detection module to overcome the limitation of false positive generation by the current method.

The auto-segmentation of calcium is very attractive for a full volumetric analysis and can indicate regions with superficial calcium in which lesion preparation may optimize or facilitate stent implantation.

Macrophages (foam cells)

Foam cells are cholesterol-engorged macrophages found both in the early stage of atherosclerotic lesions and in more advanced lesions, such as lipid-rich plaques [31]. High density macrophages are correlated with high risk of plaque rupture and associated acute coronary events [32]. Recent studies hypothesized that OCT is able to identify macrophages [5, 33, 34]. Foam cells have different refractive indexes from the surrounding extracellular matrix, representing themselves as "bright spots" under OCT. Hypothesizing that macrophages contribute to a high heterogeneity, Tearney et al. [5] used normalized standard deviation (NSD) of a selected window within the fibrous cap to quantify

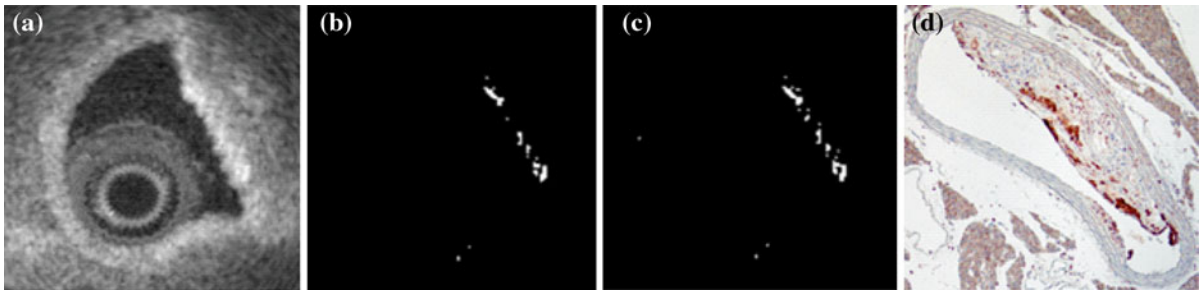

Fig. 4 Automatic segmentation of macrophages. **a** OCT image of one cross section of ApoE-/- mouse aorta containing many macrophages. Manual (**b**) and automated (**b**) segmentations considering both the intensity and normalized standard deviation with good agreement with Mac-3 stained (**d**) macrophages

macrophages. To evaluate the relationship between macrophage distribution and unstable versus stable coronary syndromes, in a later clinical study [34], "mean NSD" was used within the automatically segmented fibrous cap by bimodal histogram to quantify macrophage density. Potential limitations of this method includes that since fibrous cap may not be accurately segmented by bimodal histogram, the mean NSD may not reflect the true macrophage density within the cap. Any rapid signal changes, such as tissue boundary, could contribute to high NSD. Furthermore, whether the "bright spots" are indeed macrophages still needs more stringent validation. This is not trivial because the small size of macrophages (20–50 μm) makes the exact registration of histology and OCT difficult. Recent development of ultrahigh resolution OCT (1–5 μm) [35] may provide better opportunities for visualization of macrophages. More research needs to be done to validate the criteria for identification of macrophages by OCT and to develop robust methods for macrophage quantification. Our group is pursuing an approach that combines intensity and multi-scale standard deviation to directly segment the macrophages (Fig. 4). Ultimately Cryoimaging will provide the chance for better co-registration for macrophage validation.

Future perspective on plaque validation methodology

OCT validation

Histopathology is generally used as a validation method for OCT. The most frequently used validation method consists of standard histology techniques of paraffin embedded tissue and staining. All validation papers on OCT plaque characterization rely on this method [3, 5, 21, 36]. However, histopathology itself has limitations that must be acknowledged. Tissue loss and artifacts are significant with the saw and grinding technique, whereas sectioning artifacts, such as folding, are more frequent with the rotary microtome technique [37].

A second major challenge with histology is the difficulty in properly co-registering the histological slides to the corresponding OCT frames: side branches are mostly used to acquire the best match between an OCT cross section and its corresponding histological section [3, 5]. To be able to co-register histological slides to the corresponding OCT frames in a proper way, a wide sampling interval is used that ranges from 50 to 200 μm [4, 8, 17].

A third challenge comes with the tissue preparation: because of dehydration, shrinkage of the vessel will occur. Also, in arteries with significant amounts of calcified plaque, decalcification is mandatory. This leads to changes in tissue characteristics [3, 5, 38].

Robotic cryo-imaging

New methods are being developed to pass these limitations and allow better validation of OCT and other in vivo imaging modalities. Particularly for taking advantage of the high resolution and tissue contrast obtained with OCT, new validation methods are even more important. Among these, Robotic Cryo imaging was introduced a few years ago by our group at the Case Western Reserve University. The technique utilizes a large-specimen cryo microtome with a mounted episcope microscope and a charge-coupled

Fig. 5 Cryo-imaging apparatus. Block face images of embedded frozen tissue samples are captured with an episcopic microscope and CCD camera and processed using image processing techniques

device (CCD) camera to obtain block face images of embedded frozen tissue samples [39] (Fig. 5). Vessels to be imaged are flash frozen in an optical cutting temperature solution and mounted on the stage of the microtome. Sectioning is done at an interval of 5–40 μm, and an image of each cross section is saved in the system for post processing. The technique relies on differences in auto-fluorescence of the different components of a vessel when excited at different wavelengths. One of the advantages of cryo-imaging is its ability to preserve tissue characteristics since no fixation is needed before imaging. To allow a good assessment of plaque architecture and components, our group designed a 3-axis robotic positioner that allows very high-resolution imaging. The computer control system automatically pans the positioner over the specimen for a high-resolution tiled image acquisition [40]. Robotic Cryo-imaging has been validated for ex vivo characterization of human atherosclerotic plaques [41] (Fig. 6).

The main advantage of the Case Cryo-imaging system lies in the ability to generate 3D reconstructions of the imaged specimen [40]. The importance of such a visualization tool in the study of atherosclerotic plaques is notable. First, the ability to obtain an exact co-registration of the Cryo-imaged plaque to its OCT image becomes possible. After combining the 3D reconstruction obtained by post-processing of the Cryo images to a 3D reconstruction of the OCT images, any frame of interest on OCT can be easily assessed and compared with its exactly matching 2D frame. Assessment is then possible at a 5–40 μm interval. A second important advantage of 3D Cryo-imaging is that it allows volumetric quantification of plaque burden and plaque components.

The main limitation of Robotic Cryo-imaging at this stage is the impossibility of performing special techniques like immunohistochemistry. This limitation will mostly be solved by the new Cryo-imaging system under development at the Case Western Reserve University that will allow the collection of the imaged cross sections for techniques like immunohistochemistry.

Conclusion

Intravascular OCT has a tremendous potential of helping us in the better understanding and management of atherosclerotic disease. In particular, the potential of identifying TCFA with inflammation, place the method in a unique position for the study of vulnerable plaque. Also, precise calcium quantification may help on percutaneous intervention planning.

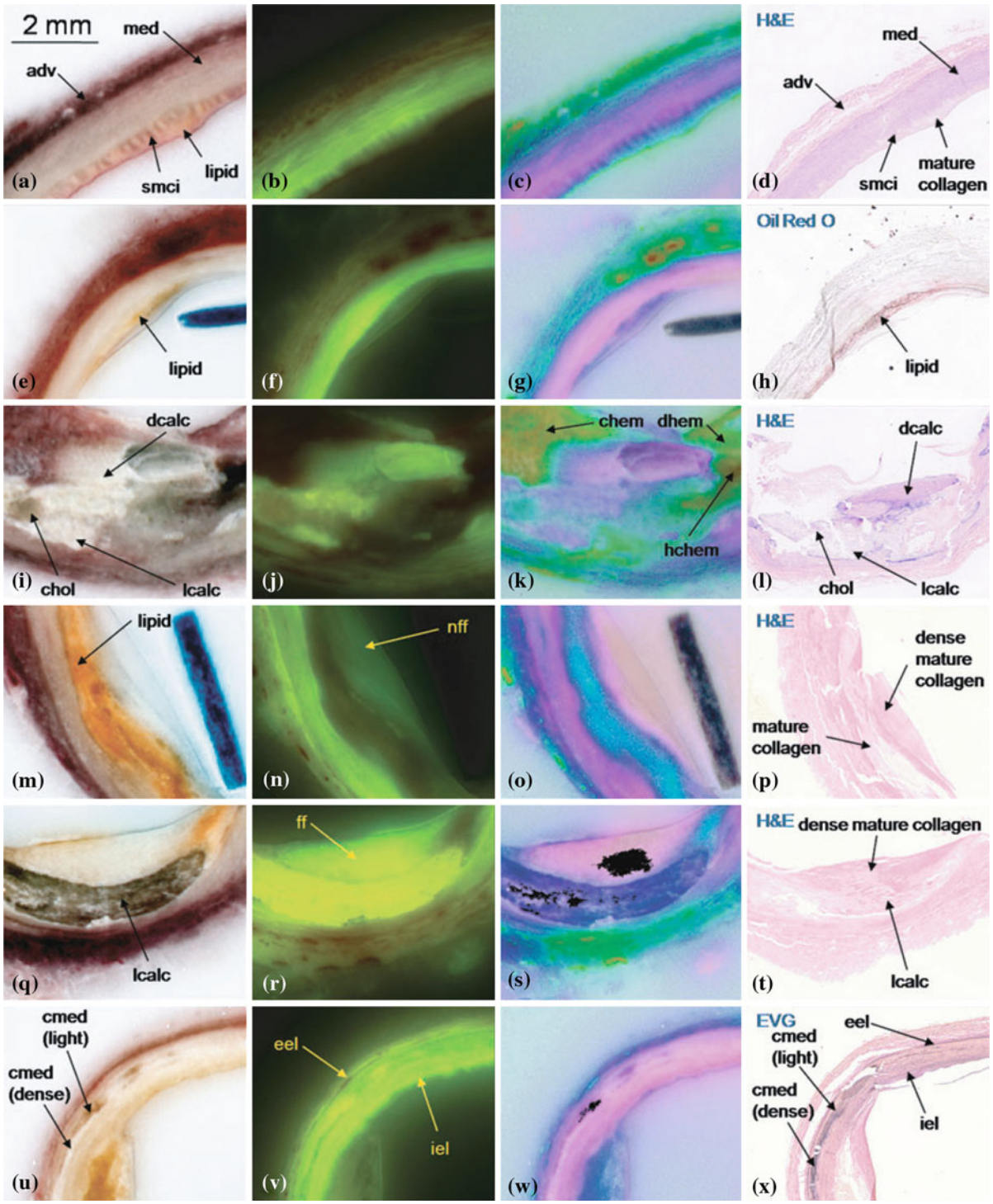

Fig. 6 Examples of each tissue type in contrast-enhanced bright-field, fluorescence, and pseudo-colour cryo-images and corresponding histology (haematoxylin and eosin, Elastic van Gieson, Mallory's trichrome and Oil Red O). The stain is shown in upper left corner of each histology panel. Images from each row are from same block face. *adv* adventitia, *med* media, *cmed* calcification in media, *smci* smooth muscle cell ingrowth, *eel* external elastic lamina, *iel* internal elastic lamina, *ff* fluorescent fibrosis, *nff* non-fluorescent fibrosis; lipid, *chol* cholesterol clefts, *lcalc* light calcification, *dcalc* dense calcification

As the method evolves, the need for more robust data on the validation process also increases. For this proposal new methods/techniques should be developed that takes in consideration better tissue preservation and high sample rates.

Conflict of interest None.

References

1. Huang D, Swanson EA, Lin CP, Schuman JS, Stinson WG, Chang W, Hee MR, Flotte T, Gregory K, Puliafito CA et al (1991) Optical coherence tomography. Science 254: 1178–1181
2. Brezinski ME, Tearney GJ, Bouma BE, Izatt JA, Hee MR, Swanson EA, Southern JF, Fujimoto JG (1996) Optical coherence tomography for optical biopsy. Properties and demonstration of vascular pathology. Circulation 93: 1206–1213
3. Yabushita H, Bouma BE, Houser SL, Aretz HT, Jang IK, Schlendorf KH, Kauffman CR, Shishkov M, Kang DH, Halpern EF, Tearney GJ (2002) Characterization of human atherosclerosis by optical coherence tomography. Circulation 106:1640–1645
4. Jang IK, Bouma BE, Kang DH, Park SJ, Park SW, Seung KB, Choi KB, Shishkov M, Schlendorf K, Pomerantsev E, Houser SL, Aretz HT, Tearney GJ (2002) Visualization of coronary atherosclerotic plaques in patients using optical coherence tomography: comparison with intravascular ultrasound. J Am Coll Cardiol 39:604–609
5. Tearney GJ, Yabushita H, Houser SL, Aretz HT, Jang IK, Schlendorf KH, Kauffman CR, Shishkov M, Halpern EF, Bouma BE (2003) Quantification of macrophage content in atherosclerotic plaques by optical coherence tomography. Circulation 107:113–119
6. Jang IK, Tearney GJ, MacNeill B, Takano M, Moselewski F, Iftima N, Shishkov M, Houser S, Aretz HT, Halpern EF, Bouma BE (2005) In vivo characterization of coronary atherosclerotic plaque by use of optical coherence tomography. Circulation 111:1551–1555
7. Rieber J, Meissner O, Babaryka G, Reim S, Oswald M, Koenig A, Schiele TM, Shapiro M, Theisen K, Reiser MF, Klauss V, Hoffmann U (2006) Diagnostic accuracy of optical coherence tomography and intravascular ultrasound for the detection and characterization of atherosclerotic plaque composition in ex vivo coronary specimens: a comparison with histology. Coron Artery Dis 17:425–430
8. Kume T, Akasaka T, Kawamoto T, Watanabe N, Toyota E, Neishi Y, Sukmawan R, Sadahira Y, Yoshida K (2006) Assessment of coronary arterial plaque by optical coherence tomography. Am J Cardiol 97:1172–1175
9. Sawada T, Shite J, Garcia-Garcia HM, Shinke T, Watanabe S, Otake H, Matsumoto D, Tanino Y, Ogasawara D, Kawamori H, Kato H, Miyoshi N, Yokoyama M, Serruys PW, Hirata K (2008) Feasibility of combined use of intravascular ultrasound radiofrequency data analysis and optical coherence tomography for detecting thin-cap fibroatheroma. Eur Heart J 29:1136–1146
10. Kubo T, Imanishi T, Takarada S, Kuroi A, Ueno S, Yamano T, Tanimoto T, Matsuo Y, Masho T, Kitabata H, Tsuda K, Tomobuchi Y, Akasaka T (2007) Assessment of culprit lesion morphology in acute myocardial infarction: Ability of optical coherence tomography compared with intravascular ultrasound and coronary angioscopy. J Am Coll Cardiol 50:933–939
11. Giattina SD, Courtney BK, Herz PR, Harman M, Shortkroff S, Stamper DL, Liu B, Fujimoto JG, Brezinski ME (2006) Assessment of coronary plaque collagen with polarization sensitive optical coherence tomography (ps-oct). Int J Cardiol 107:400–409
12. Nadkarni SK, Pierce MC, Park BH, de Boer JF, Whittaker P, Bouma BE, Bressner JE, Halpern E, Houser SL, Tearney GJ (2007) Measurement of collagen and smooth muscle cell content in atherosclerotic plaques using polarization-sensitive optical coherence tomography. J Am College Cardiol 49:1474–1481
13. Levitz D, Thrane L, Frosz M, Andersen P, Andersen C, Andersson-Engels S, Valanciunaite J, Swartling J, Hansen P (2004) Determination of optical scattering properties of highly-scattering media in optical coherence tomography images. Opt Express 12:249–259
14. van der Meer FJ, Faber DJ, Baraznji Sassoon DM, Aalders MC, Pasterkamp G, van Leeuwen TG (2005) Localized measurement of optical attenuation coefficients of atherosclerotic plaque constituents by quantitative optical coherence tomography. IEEE Trans Med Imaging 24: 1369–1376
15. Xu C, Schmitt JM, Carlier SG, Virmani R (2008) Characterization of atherosclerosis plaques by measuring both backscattering and attenuation coefficients in optical coherence tomography. J Biomed Opt 13:034003
16. van Soest G, Goderie T, Regar E, Koljenovic S, van Leenders GL, Gonzalo N, van Noorden S, Okamura T, Bouma BE, Tearney GJ, Oosterhuis JW, Serruys PW, van der Steen AF (2010) Atherosclerotic tissue characterization in vivo by optical coherence tomography attenuation imaging. J Biomed Opt 15:011105
17. Kume T, Akasaka T, Kawamoto T, Okura H, Watanabe N, Toyota E, Neishi Y, Sukmawan R, Sadahira Y, Yoshida K (2006) Measurement of the thickness of the fibrous cap by optical coherence tomography. Am Heart J 152:755 e751–754
18. Kubo T, Imanishi T, Takarada S, Kuroi A, Ueno S, Yamano T, Tanimoto T, Matsuo Y, Masho T, Kitabata H, Tanaka A, Nakamura N, Mizukoshi M, Tomobuchi Y, Akasaka T (2008) Implication of plaque color classification for assessing plaque vulnerability: a coronary angioscopy and optical coherence tomography investigation. JACC Cardiovasc Interv 1:74–80
19. Kashiwagi M, Tanaka A, Kitabata H, Tsujioka H, Kataiwa H, Komukai K, Tanimoto T, Takemoto K, Takarada S, Kubo T, Hirata K, Nakamura N, Mizukoshi M, Imanishi T, Akasaka T (2009) Feasibility of noninvasive assessment of thin-cap fibroatheroma by multidetector computed tomography. JACC Cardiovasc Imaging 2:1412–1419
20. Fujii K, Masutani M, Okumura T, Kawasaki D, Akagami T, Ezumi A, Sakoda T, Masuyama T, Ohyanagi M (2008)

Frequency and predictor of coronary thin-cap fibroatheroma in patients with acute myocardial infarction and stable angina pectoris a 3-vessel optical coherence tomography study. J Am Coll Cardiol 52:787–788
21. Kume T, Akasaka T, Kawamoto T, Ogasawara Y, Watanabe N, Toyota E, Neishi Y, Sukmawan R, Sadahira Y, Yoshida K (2006) Assessment of coronary arterial thrombus by optical coherence tomography. Am J Cardiol 97: 1713–1717
22. Wexler L, Brundage B, Crouse J, Detrano R, Fuster V, Maddahi J, Rumberger J, Stanford W, White R, Taubert K (1996) Coronary artery calcification: pathophysiology, epidemiology, imaging methods, and clinical implications. A statement for health professionals from the american heart association. Writing group. Circulation 94:1175–1192
23. Greenland P, Bonow RO, Brundage BH, Budoff MJ, Eisenberg MJ, Grundy SM, Lauer MS, Post WS, Raggi P, Redberg RF, Rodgers GP, Shaw LJ, Taylor AJ, Weintraub WS (2007) Accf/aha 2007 clinical expert consensus document on coronary artery calcium scoring by computed tomography in global cardiovascular risk assessment and in evaluation of patients with chest pain: a report of the american college of cardiology foundation clinical expert consensus task force (accf/aha writing committee to update the 2000 expert consensus document on electron beam computed tomography) developed in collaboration with the society of atherosclerosis imaging and prevention and the society of cardiovascular computed tomography. J Am Coll Cardiol 49:378–402
24. Mintz GS, Popma JJ, Pichard AD, Kent KM, Satler LF, Chuang YC, Ditrano CJ, Leon MB (1995) Patterns of calcification in coronary artery disease. A statistical analysis of intravascular ultrasound and coronary angiography in 1155 lesions. Circulation 91:1959–1965
25. Agatston AS, Janowitz WR, Hildner FJ, Zusmer NR, Viamonte M Jr, Detrano R (1990) Quantification of coronary artery calcium using ultrafast computed tomography. J Am Coll Cardiol 15:827–832
26. Carr JJ, Nelson JC, Wong ND, McNitt-Gray M, Arad Y, Jacobs DR Jr, Sidney S, Bild DE, Williams OD, Detrano RC (2005) Calcified coronary artery plaque measurement with cardiac ct in population-based studies: standardized protocol of multi-ethnic study of atherosclerosis (mesa) and coronary artery risk development in young adults (cardia) study. Radiology 234:35–43
27. Callister TQ, Cooil B, Raya SP, Lippolis NJ, Russo DJ, Raggi P (1998) Coronary artery disease: improved reproducibility of calcium scoring with an electron-beam ct volumetric method. Radiology 208:807–814
28. Mintz GS, Pichard AD, Kovach JA, Kent KM, Satler LF, Javier SP, Popma JJ, Leon MB (1994) Impact of preintervention intravascular ultrasound imaging on transcatheter treatment strategies in coronary artery disease. Am J Cardiol 73:423–430
29. Moussa I, Di Mario C, Moses J, Reimers B, Di Francesco L, Martini G, Tobis J, Colombo A (1997) Coronary stenting after rotational atherectomy in calcified and complex lesions. Angiographic and clinical follow-up results. Circulation 96:128–136
30. Wang Z, Kyono H, Bezerra HG, Wang H, Gargesha M, Alraies C, Xu C, Schmitt JM, Wilson DL, Costa MA, Rollins AM (2010) Semi-automatic segmentation and quantification of calcified plaques in intracoronary optical coherence tomography images. J Biomed Opt 15:061711
31. Lusis AJ (2000) Atherosclerosis. Nature 407:233–241
32. Moreno PR, Falk E, Palacios IF, Newell JB, Fuster V, Fallon JT (1994) Macrophage infiltration in acute coronary syndromes. Implications for plaque rupture. Circulation 90:775–778
33. MacNeill BD, Bouma BE, Yabushita H, Jang IK, Tearney GJ (2005) Intravascular optical coherence tomography: cellular imaging. J Nucl Cardiol 12:460–465
34. MacNeill BD, Jang IK, Bouma BE, Iftimia N, Takano M, Yabushita H, Shishkov M, Kauffman CR, Houser SL, Aretz HT, DeJoseph D, Halpern EF, Tearney GJ (2004) Focal and multi-focal plaque macrophage distributions in patients with acute and stable presentations of coronary artery disease. J Am Coll Cardiol 44:972–979
35. Drexler W, Morgner U, Kartner FX, Pitris C, Boppart SA, Li XD, Ippen EP, Fujimoto JG (1999) In vivo ultrahigh-resolution optical coherence tomography. Opt Lett 24: 1221–1223
36. Nadkarni SK, Pierce MC, Park BH, de Boer JF, Whittaker P, Bouma BE, Bressner JE, Halpern E, Houser SL, Tearney GJ (2007) Measurement of collagen and smooth muscle cell content in atherosclerotic plaques using polarization-sensitive optical coherence tomography. J Am Coll Cardiol 49:1474–1481
37. Bezerra HG, Costa MA (2010) Will intravascular OCT shed light on vascular biology? JACC Cardiovasc Imaging 3:85–87
38. Meissner OA, Rieber J, Babaryka G, Oswald M, Reim S, Siebert U, Redel T, Reiser M, Mueller-Lisse U (2006) Intravascular optical coherence tomography: comparison with histopathology in atherosclerotic peripheral artery specimens. J Vasc Interv Radiol 17:343–349
39. Salvado O, Roy D, Heinzel M, McKinley E, Wilson D (2006) 3d cryo-section/imaging of blood vessel lesions for validation of mri data. Proc Soc Photo Opt Instrum Eng 6142:377–386
40. Roy D, Breen M, Salvado O, Heinzel M, McKinley E, Wilson D (2006) Imaging system for creating 3d block-face cryo-images of whole mice. Proc Soc Photo Opt Instrum Eng 6143:nihpa112282
41. Nguyen MS, Salvado O, Roy D, Steyer G, Stone ME, Hoffman RD, Wilson DL (2008) Ex vivo characterization of human atherosclerotic iliac plaque components using cryo-imaging. J Microsc 232:432–441